

### Responses to reviewer #1:

Please find our responses to the review below. Original review is displayed in black, our responses in blue.

5

The study is motivated by the question, how much phosphorus is supplied to the Amazon by North African dust sources. The authors examine the source regions for winter time dust storms (as this is the season when dust is transported towards the Amazon) for three consecutive years (2015-2017). Geomorphological characteristics of the source region were determined for the ten strongest dust storms per winter season. The manuscript is well written and I enjoyed reading it. Nevertheless, I have a few questions I would like the authors to address before publication

10

Response: We would like to thank the reviewer for the assessment of the paper and for the constructive feedback and helpful questions.

15

General comments: (1) The question I am most curious to know the answer remains somewhat unanswered: Can you estimate how much phosphorus is supplied to the Amazon by the individual dust source regions? E.g., Schepanski et al., Atmos. Chem. Phys. (2009) examined by means of a model simulation the contribution of dust emitted from the Bodélé Depression to the atmospheric dust burden over the Gulf of Guinea and tropical Atlantic showing a contribution of up to 60% over the Equator region. But it remains unclear, how much dust passes through the tropical rain belt. I think it may be worth considering adding a trajectory analysis here showing how many dusty trajectories originating from an emitting dust source actually reach the Amazon without being affected by rainfall or clouds.

20

Response: We fully agree with the reviewer that this question of ‘how much phosphorus is supplied to the Amazon by the individual dust source regions?’ is an important one which needs answering. In order to do so, however, two extra key pieces of information are needed. The first is how much phosphorus is in the dust derived from the different types of sources that we identify, the second is how much of this dust reaches the Amazon (i.e. trajectory analysis, as mentioned).

25

All studies on the (fertilisation) effect of dust transport to the Amazon employ the phosphorus concentration of dust from the Bodélé Depression paleolake sediments; we do not have any information on how much phosphorus is in dust from other sources at present (e.g. other paleolakes or the paleorivers we have identified). The results from this paper show that the Bodélé is not representative of the diversity of surfaces producing dust, and so more data is needed on the phosphorus concentration in the different dust sources before this question can be answered accurately. We have sampled dust from various paleoriver and paleolake systems throughout much of Northern Africa, which we are currently analysing to get a better understanding of the phosphorus concentration in Northern African dust from the individual sources in different

30

regions. This research will be published in a follow up paper that builds on the research presented in this paper.

With regards to the trajectory analysis we again agree with the reviewer – this is a good idea. To achieve this, we are currently developing a new remote sensing trajectory analysis methodology using MODIS AOD to track dust from source to sink. This will form the basis of another follow up paper.

While we are striving to answer the questions raised by the reviewer in due course, by carrying out extensive fieldwork, lab work, and developing and testing this new remote sensing methodology for dust tracking, this involves a considerable amount of research which will be published in papers that follow on from this one. If all this research were to be combined it would form a huge paper, with multiple methods and conclusions that would bury some of the important findings.

(2) Related to question (1), how many of the identified dust sources actually contribute to the dust deposition flux over the Amazon? This can be addressed by a trajectory study as well and would be a worthy contribution to the scientific discussion on the fertilization impact of northern African dust sources

Response: This follows on from the previous question. We agree this would be a very worthy contribution to the scientific discussion, however as we would like to tackle this issue using a new remote sensing methodology in order to answer the question most accurately, we believe this would be better suited for a follow-up manuscript, to eventually be combined with our geochemical analysis of dust samples that we have collected from paleorivers and paleolakes throughout northern Africa.

(3) Was the dust mass per source region calculated for all identified dust storms originating from the corresponding location or for a selected number only? This refers to line 18-20, page 7. Please clarify. Same for the numbers provided in the results section: Are these based on all identified dust storms? Which quantities are put in relation?

Response: The dust mass per source region was calculated for all identified storms. Upon reflection this was not clearly explained (it was also mentioned by reviewer #2), and therefore we have revised the methodology section. It is now clearly stated that the selected number of dust storms (20 largest) only pertains to identifying the location of dust point sources and the classification of their geomorphology (sections 2.2 and 2.3). This has also been better clarified in the results/figures/tables.

(4) Can you please explain in more detail how the dust mass fractions were calculated (refers to line 9-12, page 9)? Providing the fraction implies you know the annual total - or at least did some assumption. Which mass fractions are related? Please clarify.

Response: The dust mass fraction is calculated as the ratio between the dust mass emitted during the 10 largest dust storms per season and the total dust mass emitted during the wintertime seasons. The total T<sub>g</sub> emitted during the 2015/2016 and 2016/2017 winter dust seasons (Dec/Jan/Feb) was 82.3 - 127.0, which can be found in Table 2. The ten largest dust storms of both seasons emitted 30.95-47.75 T<sub>g</sub>. This is how the 37.6% on line 12, page 9 (original manuscript) was calculated. As it was not clear that the values in Table 2 corresponded to all dust storms in the season, this has been clarified in both methodology and in the Table title. As per suggestion of reviewer #2, we have now split up this figure per season.

p 5, l 15-16 It is absolutely reasonable to limit the calculation to the ten strongest dust storms. Can you add a brief statement on the representativeness of the results despite this selection is made?

Response: Only with regards to the exact location of individual dust point sources and their geomorphology (methodology section 2.2 and 2.3) did we limit our methodology to the ten strongest dust storms. All other analyses were carried out for all dust storms in the seasons. Due to time constraints and labour-intensive methodology of identifying point sources and classifying geomorphology per point source we decided to limit to the ten largest dust storms per season. The representativeness of this is shown in the accuracy assessment, and the results of this can be found at lines 9-12, page 9 of the original manuscript. Nevertheless, it seems this could do with better explanation; as such we have combined these sections in a new paragraph to make it clearer (last paragraph in section 2.3 of revised manuscript).

p 7, l 19-14 Please consider referring to a map illustrating the location of the listed source regions.

Response: The map presented (in the results section of the original manuscript) illustrates the location of the listed source regions; on reflection this map was indeed better placed in the methodology section. We have moved the map and added a sentence referring to the map.

p 13, l 16 There are studies highlighting the Sudan as active dust source. E.g. Schepanski et al. (Geophys. Res. Lett. 2007, J. Geophys. Res. 2009), and Formenti et al., (Atmos. Chem. Phys., 2011).

Response: We thank the reviewer for bringing this to our attention - this was indeed an error. There are a couple of studies referring to Sudan, however these are nearly all pertaining to northern Sudan/Nubian desert. As you mention, Schepanski (2009) is the exception in naming central Sudan. We have updated this sentence to reflect we are referring to central/southern Sudan and have added Schepanski (2009).

**Responses to reviewer #2 (Ian Ashpole):**

Please find our responses to the review by Dr. Ian Ashpole below. Original review is displayed in black, our responses in blue.

5

General comments: This is an enjoyable and insightful paper that combines multiple different satellite datasets to enhance our knowledge of the geomorphology of North African dust sources and estimate how much dust is emitted from different regions. As well as being of scientific value in themselves, the results are of significance for our understanding of the fertilization link between Saharan dust and the Amazon and this case is strongly made in the paper introduction, discussion and conclusion. However, I do feel that the methods need greater clarification/explanation, and that in some places a mention of the methodological/data limitations is needed. In my opinion, this paper will be well worthy of publication once a few issues are addressed.

10

Response: We would like to sincerely thank Ian Ashpole for the thorough review and we greatly appreciate the valuable questions and suggestions.

15

My review is structured as follows: I first explain my major comment about the paper. I then outline a series of specific comments, section-by-section, which are less minor (some of these will likely be addressed in the process of addressing my major comment), before suggesting a few small technical corrections at the end.

20

My only major question/comment refers to your methods and is more a question of greater explanation/clarification needed, as opposed to me questioning the validity of what you have done (the method seems great to me, if I understand it correctly).

25

Basically, I'm not entirely clear how you get to the final results that are presented in Tables 1 and 2. From several re-reads of the methods, it is my understanding that you only classify the source geomorphology (Section 2.3) of the 20 dust events that you study in detail in Section 2.2 (using VIIRS)? Yet, in Table 1, you give the classification of 3512 sources. Does this mean that the 20 events studied originated from 3512 specific point sources in total; or does this number come from all of the events identified in the SEVIRI data (Section 2.1)? If the latter, how do you know the geomorphology of the point sources that contribute to the events that were \*not\* studied using the VIIRS data in Section 2.2 and Sentinel data in Section 2.3? (A related point: you don't state anywhere in Section 2.1 that you identify the actual sources of events identified using SEVIRI data, just that the events were "identified". If you did backtrack these events to sources, you should say so.)

30

Response: This is a very valid point. It seems the methodology section could do with greater explanation/clearer wording. We used the 20 largest dust events to determine dust point sources and the geomorphology of these dust point sources

(sections 2.2 & 2.3), all other analyses are done on ALL dust events in the wintertime seasons. In summary we use the dust point sources from the 20 largest dust storms and their geomorphology to derive the major dust sources regions. Then we assign each dust source region a predominant geomorphology. Dust plumes (all in the season) are allocated to a dust source region and assigned the predominant geomorphic class of that region. We have now added sentences in all methodology subsections to clarify this. The results section has also been updated to clarify this. It is correct that the 20 largest dust events had 3512 specific point sources in total. We did not identify the point sources of all the events identified using SEVIRI, this was done only on the 20 largest dust events.

I \*think\* the answer to the above is in the first couple of sentences of Section 2.6, but I am not 100% sure: “Analysis of the dust source locations from the 10 largest dust storms in each dust season showed that a single geomorphological source dominated in most areas. On the basis of this observation, 16 individual dust source regions were identified and mapped.” Does this mean, that all (or most of) of the events identified with SEVIRI (Section 2.1) originated from within the 16 broader regions that are outlined in Figure 3? And because you had studied in detail events that originated from these sources in the course of Sections 2.2 and 2.3, you were able to deduce the geomorphology of the whole broader area?

Response: Yes, this is correct. The dust source regions and their predominant geomorphology were determined from the location and geomorphological class of the individual dust point sources. All dust plumes identified with SEVIRI were assigned to one of the 16 broader regions based on the location of the upwind edge of the plume, and then assigned the predominant geomorphology of that region. We have revised our methodology section to make this clearer.

So, for example, if an event detected in SEVIRI that was not one of the largest 20 originated from within the boundaries of the Bodélé, it was assumed to have a source geomorphology of paleolake? If I \*am\* correct about this, then I am confused as to how you get stats in Table 1 for geomorphology types of “Sand deposits” through to “Anthropogenic”, since all of the 16 broad regions are classified as “Alluvial deposits” and/or “Paleolakes”\*. But then, some of the pins in Figure 3 (which are the sources of the 20 largest events) are colour coded to represent “Sand deposits” etc. So, do the figures in Table 1 actually only come from these top 20 events? Hopefully you can see why I am confused!

Response: The figures in Table 1 refer to the point sources of the 20 largest dust events. From the 20 largest dust events a total of 3512 individual dust point sources were identified. We have added this information in the first sentence of the results section. All these point sources were classified using the geomorphic classification scheme (e.g. Paleolake, Sand Deposit, Anthropogenic etc.). As we found that dust sources in similar regions were largely derived from the same dust source, the dust plumes which were not part of the 20 largest dust events were allocated the predominant geomorphology of the region it came from. So yes, an event detected in SEVIRI that was not one of the largest 20, which originated from within the boundaries of the Bodélé, was assumed to have a source geomorphology of paleolake. We have re-written our explanation of

this aspect of the methodology to make this clearer.

\*Relatedly: 4 of these broad regions weren't analysed as part of Sections 2.2 and 2.3 as none of the 20 biggest events originated from them: At what stage, then, did you classify their geomorphology? I think this is implied in "mapping" stage  
5 of the quoted text from the start of Section 2.6, but how you did this mapping isn't clear.

Response: When we assigned dust plumes to a region we determined 4 additional broad regions, which were not part of the 20 biggest events. At this stage we classified the geomorphology of these 4 regions using the same methods as the 20 largest dust storms. This was part of section 2.3. We have revised our methodology to include this information and clarify the  
10 process.

General: It would be helpful to clarify/be consistent with your use of the term "source" and variants ("point source", "source region", etc). In some cases you use "source" to refer to the specific point sources and features identified in Sections 2.2 and 2.3, and in other cases you use it to refer to the 16 broader source regions from Figure 3. Sometimes you use "point source"  
15 and "source regions" to refer to these, but not always.

Response: Thanks for this excellent observation, this is indeed confusing, we have corrected this such that we refer to either 'point source' or 'source region' in all cases.

20 Abstract Arguably, the first 3 sentences set this up to be a paper about fertilization, but this isn't really its focus – Amazon fertilization can only really be commented on from your (albeit quite significant) results. Can I suggest shifting these sentences to the end of the abstract/de-emphasizing the fertilization angle?

Response: The problem with this suggestion is that we only look at winter dust plumes because we are interested in dust that  
25 goes to the Amazon. If we do this, the reader will wonder why we are only looking at winter plumes, and not a full year. Given this we feel we need to explain the Amazon fertilisation angle up front. As such we have decided to not change the abstract as requested. We have, however, made it clearer that the reason why we only look at winter plumes is because we are ultimately interested in Amazon dust fertilisation.

30 1 Introduction P1, L20: Mineral dust is likely important to more parts of the earth system than just climate (i.e. biogeochemical cycles, as you emphasise this paper). You could broaden this opening statement a little to reflect this.

Response: The sentence has been replaced by: 'Mineral dust is an important component of the Earth system, affecting radiative forcing, cloud properties, and playing a key role in terrestrial, oceanic, atmospheric, and biogeochemical exchanges

(Harrison et al., 2001; Jickells et al., 2005; Mahowald et al., 2010).’

P2, L14: “While the major dust source areas within the Sahara and the Sahel have been identified. . . less is known about the geomorphology of these sources”. True, but some studies (e.g. Ashpole and Washington 2013, Crouvi et al 2012) have  
5 considered this (AW13 identifies several alluvial features as dust sources in the central and western Sahara) and could be mentioned here?

Response: We have altered the sentence to: ‘While the major dust source areas within the Sahara and the Sahel have been identified . . . , only few studies classify the geomorphology of these sources (Crouvi et al., 2012; Ashpole & Washington,  
10 2013), and knowledge of the relative importance of the major dust regions and is lacking.’

P2, L28: “. . . as well as the total dust mass emitted per class and dust source region are calculated”. Should “calculated” be changed to “estimated”, since the “calculations” contain a terms with a lot of potential error/unknowns?

15 Response: Agreed estimated is the better term, ‘calculations’ has been replaced by ‘estimated’.

#### 2.1. Detecting dust storms

Did you detect the sources of all dust events that were identified? You don’t explicitly say this, but it seems that you must have done for the later methods to make sense?

20

Response: We did not detect point sources for all dust events. We identified the region it originated from based on the upwind edge of the plume. This information has been added.

P5, L6-7: “By visually interpreting images, all dust events of the 2015-2017 boreal winter dust seasons were identified”. Did  
25 you have some subjective threshold of what was and wasn’t a dust event? From experience of working with these data I know that there are sometimes minor dust plumes that are hard to reliably trace to a specific source area. Similarly, how about when detection/interpretation/tracking was complicated by the presence of clouds? I appreciate that you do the best job you can with the data at hand and that no analysis is perfect, but I think it is important to note somewhere if you actually just identified, for example, all dust events that could be tracked to a source with confidence, since this will introduce an element  
30 of uncertainty (albeit probably small) into your results.

Response: SEVIRI was used as quick initial visual tool to observe dust storms, the actual analysis of dust mass was done using VIIRS for which the thresholds of your (Ashpole & Washington, 2012) automated dust detection technique are used (Eq. 1). Detecting dust sources under clouds is impossible with the Dust RGB technique, thus these were not included in the

study. We have added this information: ‘The individual dust plumes were tracked upwind back to their first point of occurrence (see Figure 2), except for those forming under clouds (dust storms with sources under clouds were visible on approximately 2 days per month and this was thus not a significant problem).’

5 2.2 Identifying dust sources P5, L14-15 (and also Figure 2): “Dust sources were identified manually using visual interpretation, by tracking the individual plumes back to their first point of occurrence (illustrated in Figure 2)”. I think this needs a little more explanation/clarification: The VIIRS data just show you a dust plume at a single point in time. How can you be \*sure\* what the first point of occurrence is? Is it taken as the most upwind point of the plume (with the upwind direction deduced from watching plume evolution in the SEVIRI data)? Additionally, in the example of Figure 2, you seem to have attributed the plume to 5 specific source locations, but what about the spaces in between these points, which also seem to be a shade of pink? Or is the whole upwind edge actually taken as the source location and the black points are just illustrative? OR, is this stage just narrowing down the suspected first points of occurrence so that you know what area to study for likely emissive features in a later step? Further explanation/clarification would be helpful here!

15 Response: The first point of occurrence is indeed the most upwind point of the plume. We have added this information in the manuscript for clarification (in section 2.2). The spaces in between the points are a lighter shade of pink showing dispersed dust.

P5, L16: It would be helpful to clarify whether the selection of the 10 largest dust storms per season was qualitative, or whether some other quantitative means was used to pick them (such as area covered, based on the step outlined in Section 2.4?).

Response: It is based on areal coverage. We have replaced ‘spatial extent’ for ‘areal coverage’.

25 2.3 Classifying geomorphology of dust sources General: Is it possible to include example images (or a case study) of sources meeting each classification as an additional figure (or supporting material)? I think this would help non-expert readers to understand (and visualise) the different source types.

Response: This has been added as an Appendix and a reference to the appendix has been included.

30 P6, L11-13: “To account for the spatial resolution differences between VIIRS and Sentinel-2, point sources were classified as the most prominent feature and/or most common geomorphic class within 750 m of the point source.” I find the wording a little confusing here. Does the second “point source” refer to the original point identified in the VIIRS data?

Response: Yes. This has been changed into ‘point sources were classified as the most prominent feature and/or most



common geomorphic class within 750 m of the point location determined with VIIRS'

#### 2.4 Determining dust plume area

General: 1) What happens when dust plumes detected & measured in VIIRS are the result of several smaller plumes from  
5 different sources merging? How do you apportion the plume between the different sources? Or is this never an issue?

Response: Most often individual point sources merge into one dust plume (as can be seen in Figure 2, 5 point sources – 1  
plume). We do not apportion the dust mass to a single dust point source, only to dust plumes. The dust plumes could be  
attributed to one source region with a known source geomorphology.

10

2) A problem with using VIIRS to determine dust plume area as opposed to SEVIRI is that it only gives one snapshot per  
day of dust plumes. Given that the size of plumes will change due to transport and advection, this must introduce a bias in  
your results, since if VIIRS observed the plumes at a different time of day they would be smaller or larger? This has knock-  
on effects for average plume AOD calculations and dust mass calculations. You are limited in what you can do by the data at  
15 hand, but this seems important to acknowledge. Relatedly, what time of day is the VIIRS observation actually made, and  
how does this relate to the modal emission time for the region, which I think is during the morning in this season (based on  
the work of e.g. Schepanski et al. 2009 & others)?

Response: VIIRS mean overpass time is 1.30pm local time, which coincides with MODIS Aqua data. The difference of the  
20 actual observation time between VIIRS and MODIS was <20 minutes.

We have added the overpass times and the difference in the manuscript. Most dust storms start (first observation) between  
06.00-09.00 and 09.00-12.00, with a few sources starting emission between 12.00-15.00 (Schepanski et al., 2009). However,  
we noticed that most sources emit for several hours and thus even if they initiate early in the morning they will still be  
detected by VIIRS. We found that on only 1-2 days per season a dust storm initiated after 13.30 and were hence not included  
25 in the analysis (which we also added to the manuscript). Our other AOD option would have been to use MODIS Terra, at a  
mean local overpass time of 10.30AM. The downsides of Terra compared to Aqua would be that we would have missed dust  
storms starting after 10.30AM, we would have underestimated dust storms which were still emitting between 10.30-13.30  
(this was especially common for larger dust storms), and we would have to use SEVIRI data with lower spatial resolution as  
the overpass time would not coincide with VIIRS. As such, we decided that the combination of VIIRS and MODIS Aqua  
30 was better suited.

P6, L23-24: "dust plumes could be outlined and their size calculated". For clarification, this enables you to treat each  
individual dust plume separately and assign that dust plume area to certain source?

Response: Yes. This has been clarified (section 2.3).

2.5 Measuring average aerosol optical depth per plume General: You may have clarified this in addressing my major comment, but do you get the average AOD of every dust plume identified in Section 2.1, or just the subset studied in

5 Sections 2.2 – 2.3?

Response: Has been addressed in response to major comment, but indeed, we get average AOD for all dust plumes identified in section 2.1.

10 General: How do you actually go about calculating the average AOD per plume? Is it a case of overlapping the VIIRS and MODIS data, getting all AOD values that overlap with flagged dust plumes from Section 2.4, and calculating the arithmetic mean (or median) for each individual dust plume? How do you deal with the resolution mismatch between the MODIS data (10 km) and VIIRS data (0.75 km)?

15 Response: We determine a plume boundary outline from VIIRS, this is overlapped on the MODIS data, and the arithmetic mean is calculated using statistics analysis in ENVI based on the overlapped region. The plume boundary is a georeferenced vector layer, such that resolution mismatch does not pose a problem.

P6, L31: “MODIS monitors AOD on a daily basis”. Is there any temporal offset between the MODIS and VIIRS data, or are  
20 the sensors carried on the same satellite? This seems important to me because if the plume area/mean AOD are obtained at different points in the plume lifetime, its location may have changed, which would be problematic if using VIIRS pixels to get AOD values from MODIS data. . .

Response: As mentioned before, VIIRS and MODIS Aqua have the same mean overpass time. This information has been  
25 added.

2.6 Calculating dust mass per dust source

Suggested modification for section title: “Estimating emitted dust mass per dust source region”? Terms in your calculation contain a lot of potential error/uncertainty (plume size, mean AOD, extinction coefficients. . .), so this is really more of a  
30 rough estimate. Also, you seem to consider dust mass for broader source regions as opposed to individual point sources, which is what the term “source” also occasionally refers to in this paper.

Response: We agree with the suggestion, this has been modified.

P7, L9-17: This paragraph seems like it could be better placed in its own sub-section, explaining how you pull the methods of Section 2.1 – 2.5 together to create a set of dust plumes per broad source region, as that step (if I understand your methods correctly) seems like it needs greater emphasis. However, this may not be the case depending on how you address my major comment.

- 5 P7, L9-10: “Analysis. . .showed that a single geomorphological source dominated in most areas”. Do you mean single geomorphological source class?

Response: Yes, this has been corrected.

- 10 P7, L10: “On the basis of this observation, 16 individual dust source regions were identified and mapped”. What does “and mapped” mean? Does this refer to digital boundary creation or some such to help with categorising the source area of all of the individual plumes detected in Section 2.1? I think clarification/clearer explanation is needed in this section.

Response: ‘and mapped’ refers to ‘outlined on a map’. As mentioned before, this part has been re-written and moved to section 2.3.

15

P7, L14-15: “Each dust plume was then assigned a geomorphic class based on the region it came from”. I’m confused. By “each dust plume”, are you referring to all the plumes detected in Section 2.1? If so, you didn’t state in that section that you identified sources. I am guessing this must be the case because (I think?) that you also have the size and mean AOD for all these plumes. . .

20

Response: Yes, ‘each dust plume’ refers to all plumes. As per the major question/comment this has been clarified.

- 25 P7, L15-17: “The accuracy of this methodology was evaluated by randomly selecting three additional days, analysing the geomorphic class of each source, and determining what percentage of these dust sources coincided with that defined by the map of predominant dust geomorphologies.” Suggested addition for clarity: “. . .analysing the geomorphic class of each detected dust source. . .” Additionally: does it make sense to move your statements about the accuracy assessment results from the end of Section 3 (P9, L9-11) to here? They don’t add anything to the overall paper results, and the current wording here leaves me asking the question “well. . .how accurate did your methodology turn out to be?!”

- 30 Response: Yes, that indeed makes more sense. We have moved it.

P7, L19: “. . .whereby dust mass is calculated. . .” Again, can I suggest calculated be substituted for estimated? Can I also suggest a statement be made about the reliability of these results, given all of the (presumably quite uncertain and highly variable) parameters in Kaufman’s equations, as well as the fact that you are using a plume average AOD and plume size

calculation which are taken from one snapshot through the dust event's lifetime (and these values could therefore be quite different if calculated using observations at a different time of day).

5 Response: Calculated has been substituted for estimated. We have added that the daily temporal resolution of MODIS/VIIRS is a limitation to the study in section 2.5 and put greater emphasis on the uncertainty of the Kaufman equation in section 2.6.

P8, L3: "although it should be noted that the equation has an uncertainty of  $\pm 30\%$  for AOD values between 0.2 and 0.4." Ben-Ami et al. also note that "in cases when total AOD > 0.4, the error may be larger" – this should be added.

10 Response: This has been added.

### 3 Results

General: In Table 2, you only seem to attribute dust mass to events originating from within the 16 broad source regions outlined in Figure 3. This figure shows that a small number of the point sources identified during the 20 largest dust storms that you analysed in Section 2.2 fell outside of these regions (e.g. in Egypt) and, presumably, at least a small portion of the events identified in SEVIRI data (Section 2.1) did too. If I'm right about your methodology and you calculated dust mass for all plumes, this means your "Total" mass stats (and statements about this) are missing emission from these events? Even if this is a minor proportion of the total mass emitted from the 16 main source regions, it still seems worthy of mention.

20 Response: These dust events were attributed to the nearest dust source region based on its upwind edge. This information has been added in section 2.3: 'Once the major dust source regions were established, all dust plumes of the 2015-2017 wintertime dust seasons were assigned to the nearest major source region based on its upwind edge and then assigned the predominant geomorphic class of the region they originated from'

25 P8, L19: Can you give mean AOD for the other source regions, in addition to the Bodélé Depression? It would be interesting to see whether there are significant differences between sources. For example, some source areas (such as Sudan and Ennedi, both alluvial) seem to be frequently active, but emit a comparatively small amount of dust (and the converse is true for, e.g. Algeria – paleolake). It would be interesting to know if this is a function of differences in mean AOD or plume size. Given your comments about differences in the biogeochemical make up of dust from different source geomorphologies, it seems plausible that this might in some way affect the observed AOD values from specific source types too. Alternatively, it could say something about differences in erosivity/erodibility in these regions. Either way, worthy of comment as this is useful knowledge for remote sensing/dust modelling communities (as well as others!)

Response: Thanks for the excellent suggestion, we have calculated the mean AOD per source region and incorporated this

information in Table 2.

P9, L4-5 & Table 2: A reminder (possibly just in Table 2 caption) that South Air and Erg Chech dust mass was apportioned 50/50 to the paleolake and alluvial deposit categories would be useful, as it took me a while to work out how exactly you got  
5 to the 64% & 36% numbers.

Response: The reminder has been added.

P9, L11-12: “The ten largest dust storms per season emitted 37.6% of the total dust mass.” What proportion of the total  
10 detected dust storms did the ten largest dust storms per season account for? This would be useful to know to contextualise the 37.6% figure.

Response: We have added the information per season and revised the sentence to: ‘During the 2015-2016 dust season 54.6-  
84.3 Tg of dust was emitted, of which the ten largest dust storms contributed 33.3%, while the ten largest dust storms of the  
15 2016-2017 dust season produced 45.8% of the 27.7-42.7 Tg emitted that season.’

Technical corrections (typos, citations, etc)

P5, L4: add a reference to Figure 2 (as this visualises pink dust)?

20 Response: A reference to the Dust RGB methodology? We have now added the reference to Lensky & Rosenfeld, 2008.

P5, L5: “. . .and blue the 10.8  $\mu\text{m}$  channel”. I suggest the following addition for clarity (since this is not a BTM): “. . .and  
blue the brightness temperature (BT) of the 10.8  $\mu\text{m}$  channel”.

Response: Thanks for the suggestion, we have changed this.

25

P5, L8: “[the high temporal resolution of SEVIRI] makes it suitable for observing dust storms”. I suggest the following  
addition: “[the high temporal resolution of SEVIRI] makes it suitable for observing the evolution of dust storms”. This is the  
strength of the higher temporal resolution data; you can still “observe” dust storms (or dust plumes, at least) with lower  
temporal resolution data

30

Response: This has been amended

P5, L8-9: “. . .its low spatial resolution means it is less suited to determining the location and nature of the sources”. I  
suggest the following addition: “. . .its low spatial resolution means it is less suited to determining the precise location and

nature of the sources”. The strength of the higher spatial resolution is the precision it affords, since SEVIRI can give the correct location to a scale of 3 km, no?

Response: This has been amended

5

P8, L13: “During the 2015-2017 winter dust season between 82.3 - 127.0 Tg of dust was emitted”. You should include a reference to Table 2 here.

Response: We have included the reference to Table 2.

10

P12, L15: “N and P macronutrients”. Expand abbreviations/chemical symbols?

Response: This has been corrected.

**List of all relevant changes:**

- Added a sentence to the abstract to emphasize we are analysing the wintertime months because we are interested in Amazon fertilisation
- Included two extra studies in the introduction which have looked at the geomorphology of dust sources (lines 14-16)
- Clarified methodology in introduction (lines 24-30)
- We have added sentences to the methodology to clarify that we look at the 20 largest dust storms only in sections 2.2 and 2.3 and look at all dust storms of the seasons in the other sections
- Included a limitation of methodology section 2.2 (cannot detect sources under clouds)
- Re-written section 2.3 to explain in more detail how dust point source locations and their regions were derived, and have moved Figure 3 to this section to demonstrate this
- Moved the accuracy assessment + results from section 2.6 to section 2.3
- Updated regions 1, 2, 5, and 9 in Figure 3
- Added limitations to methodology section 2.5, and emphasized uncertainties of methodology section 2.6
- Split the dust mass value from 2015-2017 into 2015-2016 and 2016-2017 in the results section
- Added mean (arithmetic mean) AOD values in Table 2
- Updated author contributions, competing interests, and acknowledgements
- Added an appendix and reference to this appendix
- Corrected typos and improved flow

# Evaluating the Relative Importance of Northern African Mineral Dust Sources Using Remote Sensing

Natalie L. Bakker<sup>1</sup>, Nick A. Drake<sup>1</sup>, Charlie S. Bristow<sup>2</sup>

<sup>1</sup> Department of Geography, King's College London, University of London, London, UK.

<sup>2</sup> Department of Earth and Planetary Sciences, Birkbeck College, University of London, London, UK

5

Correspondence to: Natalie L. Bakker (Natalie.Bakker@kcl.ac.uk)

**Abstract.** Northern African mineral dust provides the Amazon Basin with essential nutrients during boreal winter months, when the trajectory of the Saharan dust plume is towards South America. This process, however, is still poorly understood.

10 There is little understanding where the dust is coming from, and thus what the concentration of nutrients in the dust is. This information is vital to assess the impact it will have on the Amazon. In order to further our understanding of the problem, this study analyses northern African dust sources of the boreal winter dust seasons between the years 2015-2017. It utilises high spatio-temporal resolution remote sensing data from SEVIRI, MODIS, VIIRS, and Sentinel-2 to identify dust sources, classify them according to a geomorphic dust source scheme, and quantify the relative importance of source regions by calculating the total dust mass they produce. Results indicate that paleolakes emit the most dust, with the Bodélé Depression as the single largest dust source region. However, alluvial deposits also produce a substantial amount of dust. During the boreal winter dust seasons of 2015-2017, ~36% of the total dust mass emitted from northern Africa was associated with alluvial deposits, yet this geomorphic category has been relatively understudied to date. Furthermore, sand deposits were found to produce relatively little dust, in contrast to the results of other recent studies.

## 20 1 Introduction

Mineral dust is an important component of the earth system, affecting radiative forcing, cloud properties, and playing a key role in terrestrial, oceanic, atmospheric, and biogeochemical exchanges (Harrison et al., 2001; Jickells et al., 2005; Mahowald et al., 2010). The Sahara and the Sahel are the world's largest dust source regions, emitting several hundred teragrams of mineral dust yearly (Ridley et al., 2012). Most of this dust is carried over large distances and transported west and southwest across the Atlantic Ocean (Chiapello et al., 1997). During boreal summertime dust is blown by the trade winds from northern Africa towards the Caribbean, while during winter it takes a more southerly route towards the Amazon Basin. It has been suggested that this dust has a significant fertilising effect on the nutrient deficient Amazonian rainforest soils (Swap et al., 1992; Yu et al., 2015). In order to better understand past, current, and future impacts of North African mineral dust on the Amazon Basin, the biogeochemical properties of the dust need to be determined. Recently it has been shown that these

Deleted: Mineral

Deleted: from the Sahara and Sahel

Deleted: , although

Deleted: , however,

Deleted: This

Deleted: , however, that

Deleted: to

Deleted: climate

Deleted: and

Deleted: fertilizing



properties differ significantly based on the geology and geomorphology of the terrestrial source (Gross et al., 2015, 2016), and it is therefore critical to identify dust sources and their geomorphic nature precisely.

Previous dust source identification studies have used geochemistry and mineralogy of dust samples, satellite remote sensing techniques, or back trajectory analysis (Schepanski et al., 2012; Scheuven et al., 2013; Muhs et al., 2014). In the latter case, performance of trajectory models is highly dependent on the initial conditions, and it is restricted by the quality of the input data (Gebhart et al., 2005). Tracing sources using the geochemistry and mineralogy of dust samples proves difficult for Saharan dust, as samples are sporadic in time and space, and transport affects measurements in poorly understood ways (Formenti et al., 2011). Satellite remote sensing on the other hand, provides high spatio-temporal data across the region, and has been found to be an effective method of identifying dust source areas (Prospero et al., 2002; Washington et al., 2003; Schepanski et al., 2012). Notwithstanding this, many remote sensing techniques identify erroneous sources as they average both emission and transport (Prospero et al., 2002; Washington et al., 2003), and thus methods need to be adopted which only identify the site of dust emission (Schepanski et al., 2012; Ashpole & Washington, 2013).

While the major dust source areas within the Sahara and the Sahel have been identified using remote sensing (Prospero et al., 2002; Schepanski et al., 2009; Ginoux et al., 2012; Ashpole & Washington, 2013), only a few studies classify the geomorphology of these sources (Crouvi et al., 2012; Ashpole & Washington, 2013), and knowledge of the relative importance of the major dust regions and is lacking. Studies analysing the fertilisation effect of dust on the Amazon focus primarily on the impact of paleolake Bodélé (Bristow et al., 2010; Yu et al., 2015) as this has been shown to be the most important source region (Koren et al., 2006; Ben-Ami et al., 2010). Latest estimates of phosphorous input into the Amazon are based solely on the phosphorous concentration in Bodélé dust (Yu et al., 2015), but this is unlikely to reflect the diversity of the surfaces producing dust.

The aim of this study is to identify wintertime dust sources, as only this dust is transported to the Amazon. The sources are classified according to the geomorphic dust source scheme developed by Bullard et al. (2011), after which the importance of the various dust sources is quantified, and it is calculated how much dust each region produces. This is achieved through a combination of remote sensing products with different temporal and spatial resolution, to optimise the identification of dust storms, dusts source regions and the geomorphology of individual dusts sources. The Spinning Enhanced Visible and Infrared Imager (SEVIRI) dust red, green, blue (RGB) colour composite has a high temporal resolution and is used here to detect dust storms, while the Visible Infrared Imaging Radiometer Suite (VIIRS) dust RGB with higher spatial resolution is utilised to accurately determine the dust source locations. The Moderate-resolution imaging spectroradiometer (MODIS) aerosol optical depth product is employed to quantify how much dust the sources produce, and the high spatial resolution (10 m) Sentinel-2 true colour composite is used to identify the geomorphology of each source. The study examines the dust storms of the 2015-

**Deleted:** less is known about

**Deleted:** their

**Deleted:** .

**Deleted:** fertilization

**Deleted:** the

**Deleted:** identify sources,

**Deleted:** their location, the

2017 winter dust seasons. Both the number of individual dust sources of each geomorphological class, as well as the total dust mass emitted per class and dust source region are estimated.

Deleted: calculated

## 2 Methodology

Deleted: ¶

5 The study analyses northern African dust sources during boreal wintertime, defined as the area between the longitudes 20°W – 40°E and the latitudes 5°N – 40°N. The dust seasons analysed run between Dec 1<sup>st</sup> 2015 – Feb 29<sup>th</sup> 2016 and Dec 1<sup>st</sup> 2016 – Feb 28<sup>th</sup> 2017, following the wintertime dust months of Schepanski et al. (2009). Figure 1 provides a complete overview of the data and methodology.

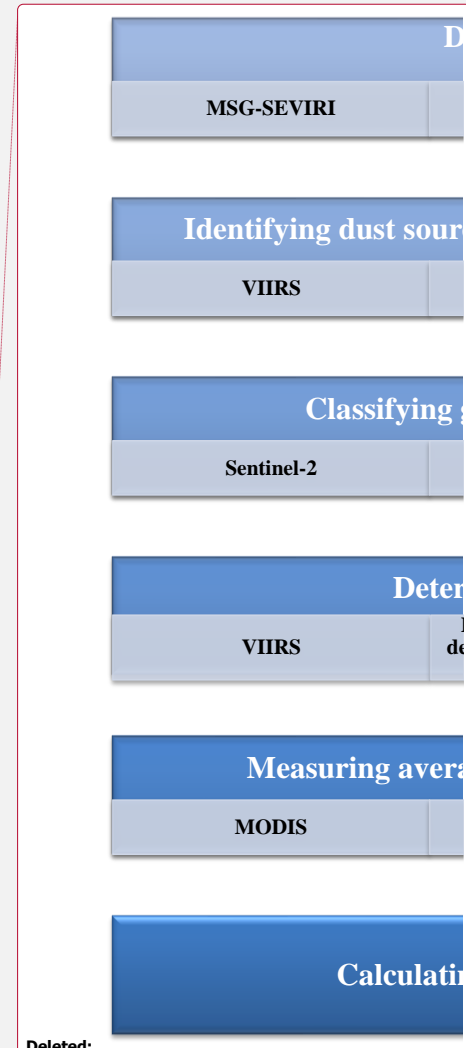
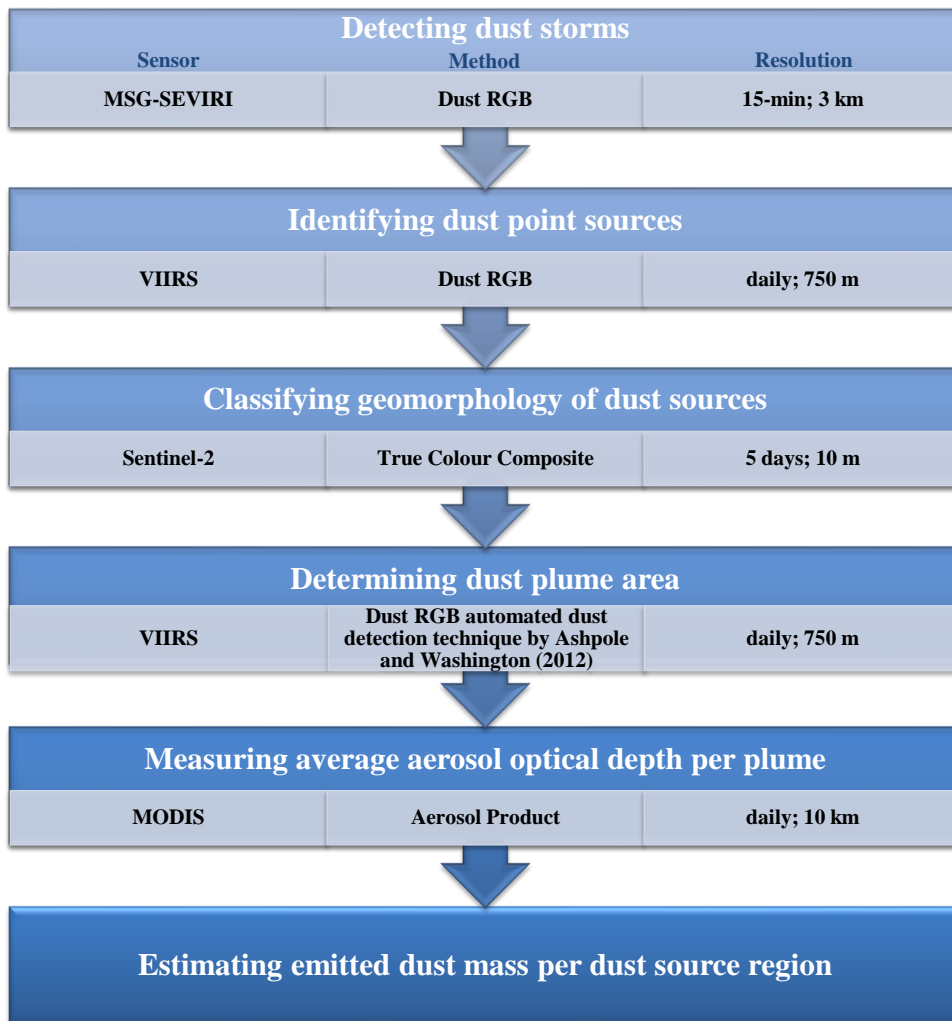


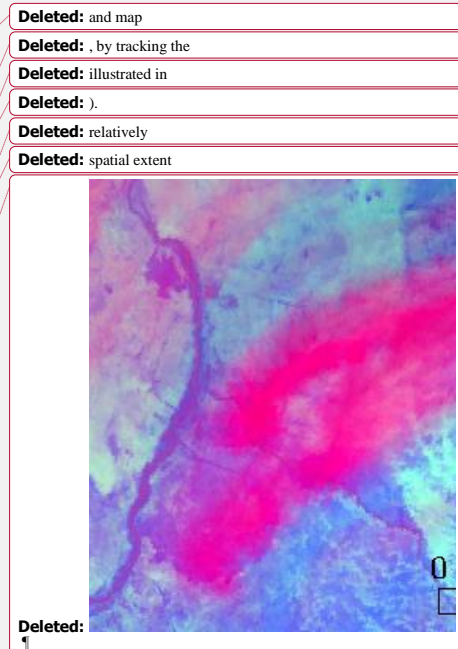
**Figure 1: Overview of the methodology of the study. The remote sensing sensor used in each step is presented in the left column, the image processing method employed is shown in the middle column, and the resolution (temporal; spatial) is shown in the right column.**

### 2.1 Detecting dust storms

5 MSG-SEVIRI was utilised to detect dust storms every 15 minutes at a spatial resolution of 3 km at nadir. The dust RGB method of Lensky and Rosenfeld (2008) was employed whereby infrared channels are utilised to produce an image in which dust is portrayed in a pink colour. To achieve this, the red band is allocated the brightness temperature difference (BTD) between channels at 12 - 10.8  $\mu\text{m}$ , green the BTD between channels at 10.8 - 8.7  $\mu\text{m}$ , and blue the brightness temperature (BT) of the 10.8  $\mu\text{m}$  channel. Processed SEVIRI dust RGB images were acquired from the database of the FENNEC project (FENNEC, 10 2017). By visually interpreting images, all dust events of the 2015-2017 boreal winter dust seasons were identified. Though the high temporal resolution of SEVIRI makes it suitable for observing the evolution of dust storms (Schepanski, 2009, 2012; Ashpole & Washington, 2012), its low spatial resolution means it is less suited to determine the precise location and nature of the sources.

### 2.2 Identifying dust point sources

15 VIIRS was used to identify dust point sources as it is currently the sensor with the highest spatial resolution that has a daily temporal resolution; it has 5 imaging-resolution bands (I-bands) at 375 m resolution, and 16 moderate-resolution bands (M-bands) at 750 m resolution. The same dust RGB method was employed using the infrared M-bands, centred at 8.55  $\mu\text{m}$ , 10.76  $\mu\text{m}$ , and 12.01  $\mu\text{m}$ . Dust point sources were identified manually using visual interpretation. The individual dust plumes were tracked upwind back to their first point of occurrence (see Figure 2), except for those forming under clouds (dust storms with sources under clouds were visible on approximately 2 days per month, and this was thus not a significant problem). As this process is labour intensive, this step was performed on only the ten largest dust storms (in areal coverage) of each dust season; i.e. a total of 20 dust storms were analysed in this step.



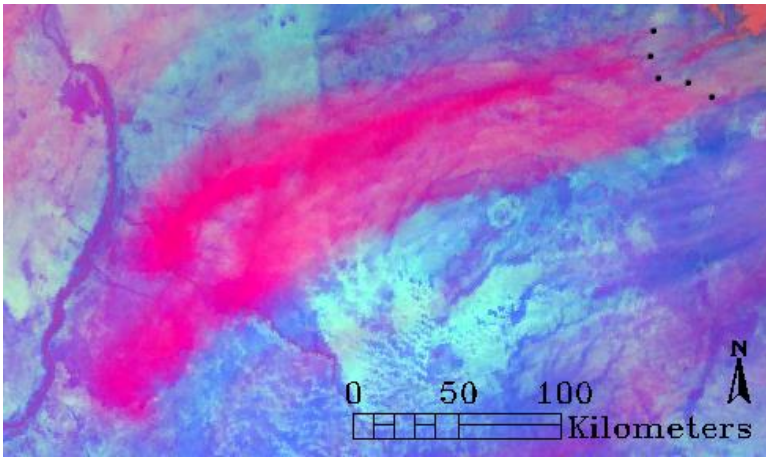


Figure 2: VIIRS Dust RGB (Lensky & Rosenfeld, 2008) showing dust being emitted northeast of the Sudanese Nile (lat: 18, lon: 35) on December 19, 2016. Dust point source locations are identified by tracking dust plumes back to their first point of occurrence.

### 2.3 Classifying geomorphology of dust sources

20 The geomorphology of the dust point sources of the 20 largest dust storms was analysed using Sentinel-2 imagery. This sensor collects visible, near infrared, and shortwave infrared imagery at a spatial resolution of 10 – 60 meters, and a temporal resolution of 5 days. Using the 10-meter resolution true colour composites, it is possible to distinguish many geomorphic features within the imagery. Cloud free, level 1c Sentinel-2 data was obtained for each of the dust point source locations identified from the VIIRS data. Each point source was interpreted and allocated to one of the geomorphic classes described

25 by Bullard et al. (2011). These classes are based on differences in surface characteristics governing their susceptibility of aeolian erosion, provided they met the criteria to be readily identifiable from remote sensing data. The classes from the scheme identified in this study are ‘paleolakes’, ‘alluvial deposits’, ‘stony surfaces’, and ‘sand deposits’. Furthermore, the class ‘anthropogenic’ was added to the classification scheme, defined as dust sources linked to urban areas, villages, roads, and agricultural lands. Examples of the various geomorphic classes can be found in Appendix i. Drake et al. (2008)

30 demonstrated that the geomorphic classification scheme could characterise dust sources in the Western Sahara region successfully. To account for the spatial resolution differences between VIIRS and Sentinel-2, point sources were classified as the most prominent feature and/or most common geomorphic class within 750 m of the point location determined with VIIRS.

Deleted: 2:

Formatted: Caption

Deleted: (black points)

Formatted: Font: Not Bold

Deleted: To determine the

Formatted: Left

Deleted: individual

Deleted: .

Deleted: was used. The

Deleted: source.

Formatted: Highlight

The identified point sources tended to spatially cluster according to their geomorphological type into 12 major dust source regions (Figure 3). In most regions, a single geomorphological source class dominated, and a predominant geomorphology per region could be determined. In two cases, namely in the South Air and El Eglab dust source regions, there was no single predominant geomorphic class, and they were thus classified as mixed paleolake and alluvial deposit (50/50%). Once the major dust source regions were established, all dust plumes of the 2015-2017 wintertime dust seasons were assigned to the nearest major source region based on its upwind edge and then assigned the predominant geomorphic class of the region they originated from. A further four prominent dust source regions were added (see regions with dashed outlines in Figure 3), which emitted dust plumes during the two winter dust seasons, although they did not emit during the 20 largest dust storms. The predominant geomorphology of these regions was determined separately through visual interpretation of Sentinel-2 data using the same methods that were employed for the 20 largest dust storms.

The accuracy of using only the 20 largest dust storm days of the two seasons to determine the major dust regions and their predominant geomorphology was evaluated by randomly selecting three additional days (29 Dec 2015, 21 Jan 2017, 8 Feb 2017), identifying all point sources of these days, analysing the geomorphic class of each detected point source, and subsequently determining what percentage of these dust point sources coincided with that defined by the map of predominant dust geomorphologies. The geomorphological class of a further 163 dust point sources were identified from the three randomly chosen days. Of the 163 dust point sources, 161 (98.77%) corresponded with the predominant geomorphology assigned to the region.



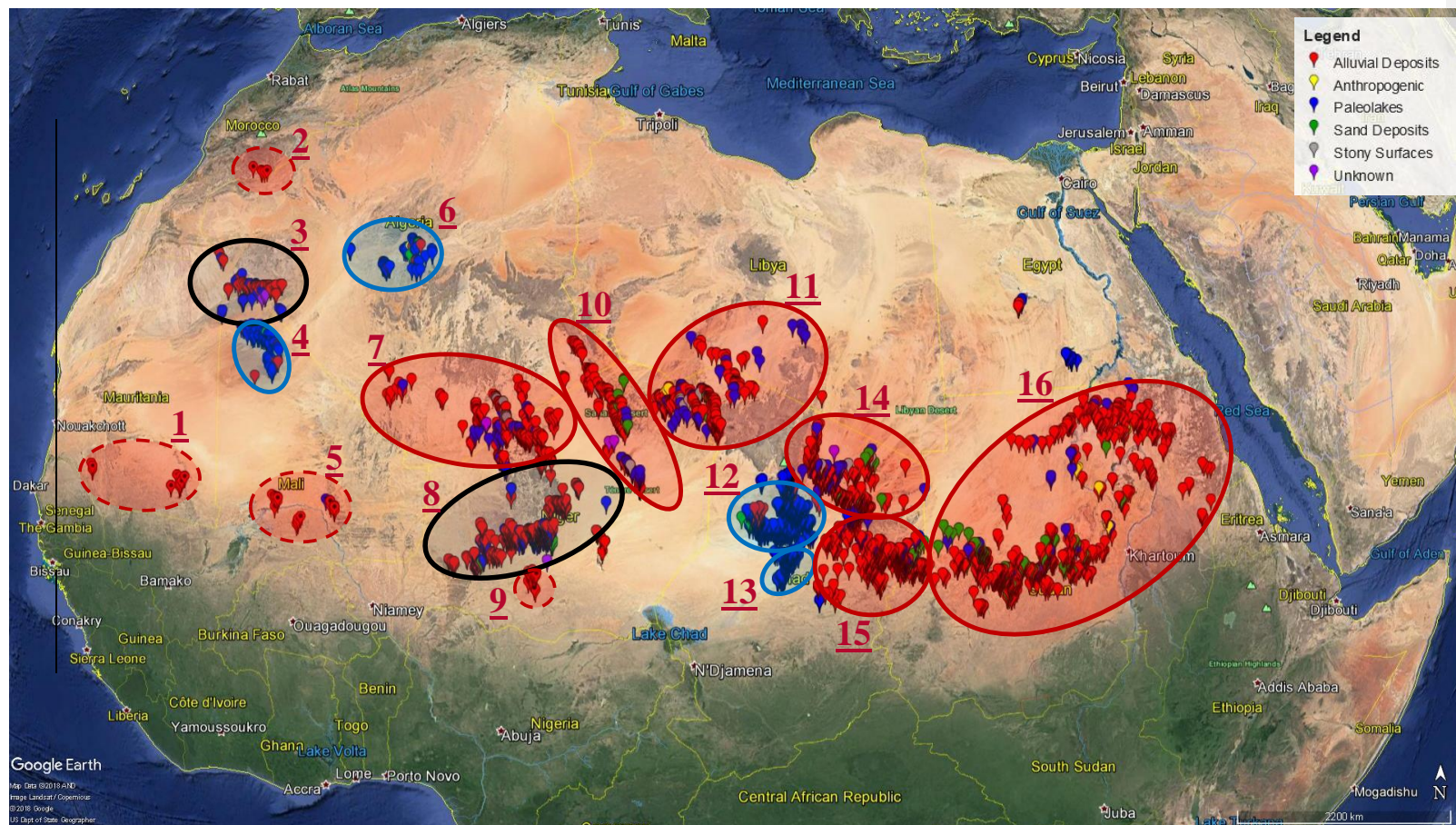


**Figure 3. Geomorphology of the northern African mineral dust sources of the 2015-2017 boreal winter dust seasons. Coloured pins represent individual dust point sources of the 20 largest dust storms of the 2015-2017 winter dust seasons, with the colour signifying the geomorphic category of the dust point source. The major dust source regions are outlined, with red regions containing predominantly alluvial deposit dust sources, blue regions containing predominantly paleolake dust sources, and black regions containing a mixture of alluvial deposit and paleolake dust sources. The regions with dashed outlines were regions that emitted dust during the dust seasons, but did not emit during the 20 largest dust storms of the 2015-2017 winter dust seasons. Source areas are numbered as follows: 1, Mauritania; 2, Draa River; 3, El Eglab; 4, Northwest Mali; 5, Mfid Mali; 6, Algeria; 7, North Air; 8, South Air; 9, South Niger; 10, Djado Plateau; 11, Tibesti; 12, Bodélé; 13, Bahr el Gazel; 14, Upper Bodélé; 15, Ennedi; 16, Sudan. Background Google Earth, imagery Landsat/Copernicus (2018).**

Moved (insert  
 Moved (insert  
 Moved (insert

## 2.4 Determining dust plume area

After the main dust source regions were determined, the next step was to estimate how much dust was emitted per region. To do so, firstly, the dust plume area was calculated for all dust plumes of the 2015-2017 wintertime dust seasons using the automated dust detection technique developed by Ashpole and Washington (2012). In this method, the following thresholds are applied to the brightness temperatures (in Kelvin) of the 10.76, 12.01, and 8.55  $\mu\text{m}$  channels of VIIRS imagery:

$$BT_{10.76} \geq 285$$

$$BTD_{(12.01-10.76)} \geq 0$$

$$BTD_{(10.76-8.55)} \leq 10$$

Background surface features that were incorrectly detected as dust were removed manually, after which dust plumes could be outlined and their size calculated. The methodology is objective, easily reproducible, fast, and was found to be consistent for moderate-to-heavy dust storms occurring during daytime hours (Ashpole & Washington, 2012). The method was applied to VIIRS, rather than SEVIRI or MODIS, due to its higher spatial resolution and its seamless continuation between swaths.

## 2.5 Measuring average aerosol optical depth per plume

In order to determine the concentration of dust within the dust plumes, average (arithmetic mean) aerosol optical depth (AOD) per dust plume was calculated for all dust storms of the 2015-2017 wintertime seasons. As the VIIRS AOD product was found to contain large data gaps, particularly over bright desert surfaces, the MODIS aerosol product (MOD04\_L2, MYD04\_L2) was employed. MODIS monitors AOD on a daily basis at a 10-km spatial resolution, and combines the MODIS Dark Target (Kaufman et al., 1997; Levy et al., 2013) and MODIS Deep Blue (Hsu et al., 2004) algorithms. MODIS Dark Target uses the spectral radiances between 0.47 and 2.1  $\mu\text{m}$  to measure AOD over oceans and dark land surfaces. MODIS Deep Blue is designed to analyse aerosols over bright-reflecting surfaces, such as deserts, utilising measurements from the blue wavelengths (412 and 470 nm). The combined algorithms allow MODIS to record data across North Africa consistently (Sayer et al., 2013).

The methodology presented here does have a few limitations. These are: 1) The once daily temporal resolution of MODIS, as dust storms in northern Africa can form during any time of the day (Schepanski et al., 2012), and this thus causes a few dust storms to be missed. Nevertheless, the vast majority of dust storms in northern Africa initiate in the morning between the hours of 06.00-12.00 (Schepanski et al., 2009), and the dust storms in this study were observed to span several hours, such that the MODIS mean overpass time of 13.30 local time did cover nearly all dust emissions; albeit dust plumes emitting after 13.30 were missed (which occurred on 1-2 days per season). 2) The MODIS and VIIRS overpass times are close but not identical, varying up to 20 minutes. 3) Dust storm days between 19-27 February 2016 had to be omitted from this study due to a MODIS technical outage, during which the satellite did not log any data, and there was hence no MODIS AOD data available.

Deleted: The

Deleted: storms in the season

Deleted: <object>

(1)

Deleted: ¶

Deleted: utilizing

Deleted: It should be noted that dust storm days between 19-27 February 2016 were



## 2.6 Estimating emitted dust mass per dust source region

The dust mass for all dust plumes of the 2015-2017 wintertime seasons was estimated by combining the dust plume area data with the average MODIS AOD. The dust column concentration equation by Kaufman et al. (2005) was applied to all dust storms, whereby dust mass is determined using the relationship between plume size and average dust AOD at 550  $\mu\text{m}$ :

$$M_{du} = 2.7A\tau_{du} \quad (2)$$

where  $M_{du}$  is dust mass,  $A$  is the dust plume area, and  $\tau_{du}$  is the average AOD at 550  $\mu\text{m}$ . The coefficient of 2.7 is derived through the extinction efficiency of 0.37 measured by Haywood et al. (2003). However, a more recent review of mass extinction efficiency measurements by Ansmann et al. (2012) shows higher reported values ranging between 0.37- 0.57. An updated Kaufman equation was derived using the extinction efficiency of 0.57, resulting in a coefficient of 1.75:

$$M_{du} = 1.75A\tau_{du} \quad (3)$$

Using equations 2 and 3, the dust mass range was estimated (i.e. eq. 3 for the lower limit, eq. 2 for the upper limit). Ben-Ami et al. (2010) demonstrated that the Kaufman equation could successfully be used to calculate dust mass over northern Africa, although it should be noted that the equation has a relatively high uncertainty of  $\pm 30\%$  for AOD values between 0.2 and 0.4, and has potentially even greater errors for AOD values above 0.4.

Once the dust mass per dust plume was estimated, dust plumes were grouped per dust source region and per geomorphology, and as such the total dust mass per region and dust mass per geomorphic class could be estimated.

## 3 Results

From the 20 largest dust storms, a total of 3512 individual dust point sources were identified (see Figure 3). The dust point sources per geomorphological class are shown in Table 1; the vast majority were associated to alluvial deposits (51.11%) or paleolakes (42.85%). Sand deposits, including dune fields and sand sheets, accounted for only 3.93%. A few sources were linked to anthropogenic influences, such as villages, dirt roads, or agricultural fields. Moreover, 22 point sources had no clear distinguishable features to place them in one of the geomorphic categories, and were thus labelled as 'unknown'.

Deleted: Calculating

Deleted: Analysis of the dust source locations from the 10 largest dust storms in each dust season showed that a single geomorphological source dominated in most areas. On the basis of this observation, 16 individual dust source regions were identified and mapped. For instance, regions of predominantly paleolake origin were the Bodélé, Bahr el Gazel, and Algeria, and those of predominantly alluvial deposit origin were the Ennedi, Sudan, North Air, and Tibesti. The South Air and El Eglab regions consisted of a substantial amount of both paleolake and alluvial dust sources in roughly equal amounts, therefore in dust mass calculations it was considered as 50% paleolake, 50% alluvial deposit. Each dust plume was then assigned a geomorphic class based on the region it came from. The accuracy of this methodology was evaluated by randomly selecting three additional days, analysing the geomorphic class of each source, and determining what percentage of these dust sources coincided with that defined by the map of predominant dust geomorphologies.¶  
<object>The dust mass per source region was determined

Deleted: calculated

Deleted: <object>

Deleted: ), however

Deleted:

Deleted: calculated

Deleted: an

Deleted: .

Deleted: A

Deleted: Fig.

Deleted: only

Deleted: % of the dust storms.

Table 1. Northern African mineral dust **point** sources of the 2015-2017 winter dust seasons classified by geomorphology type.

DUST <b>POINT</b> SOURCE GEOMORPHOLOGY TYPE	COUNT 15-16	%	COUNT 16-17	%	TOTAL COUNT	% OF TOTAL
Alluvial deposits	1293	53.47	502	45.89	1795	51.11
Paleolakes	992	41.03	513	46.89	1505	42.85
Sand deposits	82	3.39	56	5.12	138	3.93
Stony surfaces	19	0.79	15	1.37	34	0.97
Unknown	18	0.74	4	0.37	22	0.63
Anthropogenic	14	0.58	4	0.37	18	0.51
<b>TOTAL</b>	<b>2418</b>		<b>1094</b>		<b>3512</b>	

During the 2015-2017 winter dust seasons a total of between 82.3 - 127.0 Tg of dust was emitted (see Table 2). During the 2015-2016 dust season 54.6-84.3 Tg of dust was emitted, of which the ten largest dust storms contributed 33.3%, while the ten largest dust storms of the 2016-2017 dust season produced 45.8% of the 27.7-42.7 Tg emitted that season. The 2015-2016 dust season was significantly more dusty, producing approximately twice the amount of dust compared to the 2016-2017 dust season, which is also reflected in the amount of individual dust **point** sources identified per season in Table 1. The distribution of the dust over the various regions was, however, relatively similar in both seasons.

Table 2 shows the distribution of the emitted dust per dust source region, along with the frequency of emission, i.e. the percentage of days during which the region **was** an active dust source, **the mean AOD**, and the predominant geomorphology. The Bodélé Depression is identified as the single largest source region, emitting 44.5% of the dust mass, and producing the densest dust plumes with an average (arithmetic mean) AOD value of 0.91. The Bodélé, Bahr el Gazel, and Ennedi regions were the most frequently emitting dust source regions, all of them emitting during more than half of the days of the wintertime dust season. Mauritania and South Niger were the least active regions, emitting dust on only 2 of the 172 days analysed.

Dust source regions of predominantly paleolake origin emitted approximately 64% of the total dust mass during the 2015-2017 winter dust seasons, compared to 36% for the dust regions governed by alluvial influence, (note that South Air and El Eglab are counted as 50% paleolake and 50% alluvial deposit). The importance of paleolakes and alluvial deposits, however, fluctuated considerably. Figure 4 compares the influence of paleolakes versus alluvial deposits for the ten largest dust storms of the 2016-2017 winter dust season, which demonstrates this variability.

Formatted: Position: Vertical: 1.81 cm, Relative to: Page

Formatted Table

Formatted: Position: Vertical: 1.81 cm, Relative to: Page

Formatted: Position: Vertical: 1.81 cm, Relative to: Page

Formatted Table

Formatted: Position: Vertical: 1.81 cm, Relative to: Page

Formatted: Position: Vertical: 1.81 cm, Relative to: Page

Formatted Table

Formatted: Position: Vertical: 1.81 cm, Relative to: Page

Formatted: Position: Vertical: 1.81 cm, Relative to: Page

Formatted Table

Formatted: Position: Vertical: 1.81 cm, Relative to: Page

Deleted: season between 82.3 - 127.0 Tg of dust was emitted.

Deleted: full

Deleted: is

Deleted: 92

Deleted: .

Deleted: For the accuracy assessment, the geomorphological class of a further 163 dust sources were identified from the three randomly chosen days (29 Dec 2015, 21 Jan 2017, 8 Feb 2017). Of the 163 dust sources, 161 (98.77%) corresponded with the predominant geomorphology assigned to the region. The ten largest dust storms per season emitted 37.6% of the total dust mass.

.....Section Break (Next Page).....

¶ ¶

¶ ¶ ¶

¶ ¶ ¶

¶ ¶

...

Moved up [1]: Geomorphology of the northern African mineral dust sources of the 2015-2017 boreal winter dust seasons.

Deleted: Coloured pins represent individual dust sources of the ten largest dust storms during the 2015-2017 winter dust seasons.

Moved up [2]: The major dust source regions are outlined, with red regions containing predominantly alluvial deposit dust

Deleted: The striped regions were regions that emitted dust during the dust seasons, but did not emit during the ten largest dust storms.

Moved up [3]: Source areas are numbered as follows: 1, Mauritania; 2, Draa River; 3, El Eglab; 4, Northwest Mali; 5, South Niger.

Deleted: ¶

...

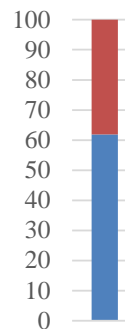
5 **Table 2. Total dust mass emitted per Saharan dust source region during the 2015-2017 winter dust seasons, alongside their predominant geomorphology, mean AOD, and their frequency of emission.**

	<u>TG 15-16</u>	<u>TG 16-17</u>	<u>TG TOTAL</u>	<u>% OF TOTAL</u>	<u>FREQUENCY (% DAYS ACTIVE)</u>	<u>MEAN AOD</u>	<u>PREDOMINANT GEOMORPHOLOGY</u>
<u>Bodélé</u>	<u>24.7 - 38.1</u>	<u>11.9 - 18.4</u>	<u>36.6 - 56.5</u>	<u>44.5</u>	<u>67.4</u>	<u>0.91</u>	<u>Paleolake</u>
<u>Bahr el Gazel</u>	<u>5.9 - 9.2</u>	<u>2.8-4.3</u>	<u>8.7 - 13.5</u>	<u>10.6</u>	<u>55.2</u>	<u>0.74</u>	<u>Paleolake</u>
<u>South Air</u>	<u>5.0 - 7.8</u>	<u>3.3-5.0</u>	<u>8.3 - 12.8</u>	<u>10.1</u>	<u>43.6</u>	<u>0.40</u>	<u>Alluvial Deposit/ Paleolake</u>
<u>North Air</u>	<u>5.3-8.2</u>	<u>1.5-2.3</u>	<u>6.8 - 10.5</u>	<u>8.3</u>	<u>25.0</u>	<u>0.31</u>	<u>Alluvial Deposit</u>
<u>Sudan</u>	<u>4.6-7.0</u>	<u>1.6-2.5</u>	<u>6.2 - 9.5</u>	<u>7.5</u>	<u>36.6</u>	<u>0.19</u>	<u>Alluvial Deposit</u>
<u>Ennedi</u>	<u>2.7-4.2</u>	<u>2.1-3.2</u>	<u>4.8 - 7.4</u>	<u>5.8</u>	<u>54.7</u>	<u>0.28</u>	<u>Alluvial Deposit</u>
<u>Algeria</u>	<u>1.3-2.0</u>	<u>1.1-1.7</u>	<u>2.4 - 3.7</u>	<u>2.9</u>	<u>12.8</u>	<u>0.32</u>	<u>Paleolake</u>
<u>Tibesti</u>	<u>1.8-2.7</u>	<u>0.6-1.0</u>	<u>2.4 - 3.7</u>	<u>2.9</u>	<u>24.4</u>	<u>0.25</u>	<u>Alluvial Deposit</u>
<u>Djado Plateau</u>	<u>1.1-1.7</u>	<u>0.4-0.7</u>	<u>1.5 - 2.4</u>	<u>1.9</u>	<u>12.2</u>	<u>0.37</u>	<u>Alluvial Deposit</u>
<u>El Eglab</u>	<u>0.4-0.6</u>	<u>0.7-1.0</u>	<u>1.1 - 1.6</u>	<u>1.3</u>	<u>5.2</u>	<u>0.35</u>	<u>Alluvial Deposit/ Paleolake</u>
<u>Mid Mali</u>	<u>0.1-0.2</u>	<u>0.8-1.2</u>	<u>0.9 - 1.4</u>	<u>1.1</u>	<u>4.7</u>	<u>0.42</u>	<u>Alluvial Deposit</u>
<u>Upper Bodélé</u>	<u>0.6-0.9</u>	<u>0.2-0.4</u>	<u>0.8 - 1.3</u>	<u>1.0</u>	<u>22.7</u>	<u>0.22</u>	<u>Alluvial Deposit</u>
<u>Draa River</u>	<u>0.7-1.0</u>	<u>0</u>	<u>0.7 - 1.0</u>	<u>0.8</u>	<u>1.7</u>	<u>0.31</u>	<u>Alluvial Deposit</u>
<u>South Niger</u>	<u>0</u>	<u>0.5-0.8</u>	<u>0.5 - 0.8</u>	<u>0.6</u>	<u>1.2</u>	<u>0.65</u>	<u>Alluvial Deposit</u>
<u>Mauritania</u>	<u>0.3-0.5</u>	<u>0.1-0.1</u>	<u>0.4 - 0.6</u>	<u>0.5</u>	<u>1.2</u>	<u>0.54</u>	<u>Alluvial Deposit</u>
<u>Northwest Mali</u>	<u>0.1-0.2</u>	<u>0.1-0.1</u>	<u>0.2 - 0.3</u>	<u>0.2</u>	<u>2.3</u>	<u>0.36</u>	<u>Paleolake</u>
<b><u>TOTAL</u></b>	<b><u>54.6-84.3</u></b>	<b><u>27.7-42.7</u></b>	<b><u>82.3 - 127.0</u></b>				

Field Code Ch

Deleted: ¶

¶



19-Dec-16  
24-D

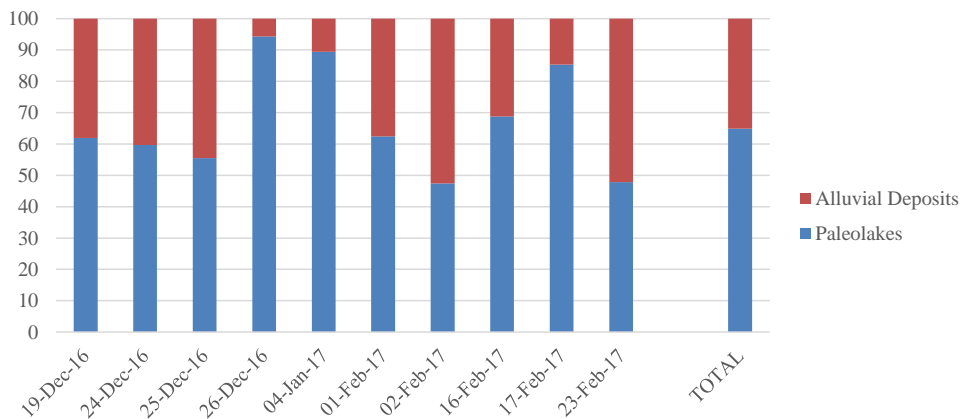


Figure 4. Contribution (in %) of paleolake dust sources versus alluvial deposit dust sources to total dust mass for the ten largest dust storm events of the 2016-2017 winter dust season.

#### 4 Discussion

##### 4.1 Paleolake and alluvial deposit dust sources

Our results indicate the importance of both paleolakes and alluvial deposits as African mineral dust sources. Alluvial deposits were found to deflate more often, while paleolakes produced more dust by emitting denser dust plumes. Dry lakebeds, most notably the Bodélé Depression, are widely known to be preferential dust sources (Prospero et al., 2002; Tegen et al., 2002). Alluvial deposits, however, have been recognised to a much lesser extent in dust source studies, especially when compared to paleolakes (Bullard et al., 2011). Producing 51.11% of the individual dust plumes and representing ~36% of the total dust mass, alluvial deposits make a significant contribution to the dust burden. Despite this, the latest estimates of the fertilisation effect of dust on the Amazon by Yu et al. (2015) determine total phosphorus deposition into the Amazon (0.022 Tg per annum) based solely on the phosphorous concentration in Bodélé dust, while not taking alluvial deposit dust sources into account. Given the fact that it has recently been shown that there are significant differences of bioavailable phosphorous content within dust from different source geomorphologies (Gross et al., 2015; 2016), and the evidence presented here of alluvial deposits being important sources, the accuracy of Yu et al.'s (2015) estimate can be questioned. In Namibia, Dansie et al. (2017) established that alluvial dust source sediments contained up to 43 times greater concentrations of bioavailable iron and enriched nitrogen (N) and phosphorus (P) macronutrients compared to paleolake pan sediments. Further research into the actual differences in nutrient content of the different northern African dust sources and dust source geomorphologies is needed to improve the precision of fertilisation estimates. This is particularly the case for the underexamined alluvial source regions.

Deleted: .....Section Break (Next Page).....

#### 4.2 Sand dunes producing dust?

While paleolakes and alluvial deposits accounted for over 90% of the emitted dust, sand deposits only accounted for 3.93%. This contradicts recent results by Crouvi et al. (2012), who found that active sand dunes were the most frequent dust sources within the Sahara. The discrepancy between the results presented here and those found by Crouvi et al. (2012) is most likely explained by the type of data used and the difference in their spatial resolution. Crouvi et al. (2012) mapped dust sources onto a coarse resolution (1° x 1°) grid, and compared them to a map of soils. When more than one soil type was present in a grid cell, Crouvi et al. (2012) assigned it to the geomorphic unit with the highest areal coverage. This carries a large bias towards widespread sand sheets and dune fields, whereas for instance paleorivers and small to medium-sized paleolakes (which could be picked up with the high-resolution Sentinel-2 data utilised in this study) are underrepresented and easily overlooked. Another major difference between the studies is that Crouvi et al. (2012) classify the Bodélé region as sand dunes, whereas in this study it is classified as a paleolake. While dunes exist in the Bodélé Depression, they are commonly composed of fragments of lake sediments and the dunes themselves are subordinate in cover to lake sediment exposures (Bristow et al., 2009). Furthermore, Crouvi et al. (2012) identified quartz-rich sand dune fields surrounding the Bodélé Depression as a major source of dust, however closer examination of the dust sources in this region, using high resolution data from VIIRS and Sentinel-2, showed this was not the case. The higher resolution data used in this study has improved the accuracy of dust source identification, and suggests that sand dunes produce little dust in northern Africa during wintertime.

#### 4.3 Location of dust sources

The majority of the locations of dust sources identified in this study correspond with previous studies such as Prospero et al. (2002), Schepanski et al. (2007; 2009; 2012), Ginoux et al. (2012), and Knippertz and Todd (2012). However, one area that has not been widely recognised as a major source region in central/southern Sudan; only Schepanski (2009) mentions this region. In southern Sudan, a few of the sources lie within the Sahel, but most are located in the Sahara. While various studies have analysed Sahelian dust emissions (Klose et al., 2010; Bergametti et al., 2017; Kim et al., 2017), less is known about the importance of the Sahel compared to the Sahara. From our data, we find that the Sahelian dust sources account for a mere 5%, with the vast majority of wintertime dust sources being located in the Sahara. Of the Sahelian dust sources, 87% are alluvial. The lack of lacustrine dust sources in the Sahel may be due to higher rainfall leading to moisture accumulation in the lake basins, which in turn suppresses dust production. The inundation of ephemeral lakes has previously been observed to lower dust emissions in semi-arid regions (Mahowald et al., 2006).

**Deleted:** - despite representing ~7.5% of dust emitted -,

#### 5 Conclusion

This study provides a quantitative analysis of wintertime northern African mineral dust sources. It outlines a novel methodology in which high temporal resolution remote sensing data is combined with high spatial resolution data to analyse

dust sources more accurately than previous dust source studies. The results show for the first time the strong importance of alluvial deposits, while simultaneously reaffirming the importance of paleolake sources. Sand deposits, on the other hand, are found to produce relatively little dust. The results concur with previous studies that the Bodélé Depression is the single largest dust source region, yet also highlight that there are lesser studied regions, such as central Sudan, producing a substantial amount of dust. It furthermore stresses the significance of the Sahara over the Sahel regarding dust production, with 95% of dust sources emitting from the Sahara.

#### Author contributions

The conceptualisation and methodology of this research was established by N.L. Bakker and N.A. Drake. Investigation and formal analysis were carried out by N.L. Bakker, supervised by N.A. Drake and C.S. Bristow. Interpretation of results determined from discussions with all three authors. The original draft of the manuscript was written by N.L. Bakker, then reviewed and edited by N.A. Drake and C.S. Bristow.

#### Competing interests

The authors declare that they have no conflict of interest.

#### Acknowledgements

This research was carried out under Natural Environment Research Council grant NE/L002485/1. The authors would like to thank Dr. Ian Ashpole and anonymous referees for reviewing the paper and providing valuable comments and suggestions.

#### **References**

Ansmann, A., Seifert, P., Tesche, M. and Wandinger, U.: Atmospheric Chemistry and Physics Profiling of fine and coarse particle mass: case studies of Saharan dust and Eyjafjallajökull/Grimsvötn volcanic plumes, *Atmos. Chem. Phys.*, 12, 9399–9415, doi:10.5194/acp-12-9399-2012, 2012.

Ashpole, I. and Washington, R.: An automated dust detection using SEVIRI: A multiyear climatology of summertime dustiness in the central and western Sahara, *J. Geophys. Res. Atmos.*, 117(D8), doi:10.1029/2011JD016845, 2012.

Ashpole, I. and Washington, R.: A new high-resolution central and western Saharan summertime dust source map from automated satellite dust plume tracking, *J. Geophys. Res. Atmos.*, 118(13), 6981–6995, doi:10.1002/jgrd.50554, 2013.

Ben-Ami, Y., Koren, I., Rudich, Y., Artaxo, P., Martin, S. T. and Andreae, M. O.: Transport of North African dust from the

**Formatted:** Font: Not Bold, Italic

**Deleted:** Conceptualisation

**Deleted:** all authors.

**Deleted:** Original

**Deleted:** review

**Deleted:** editing of manuscript

**Deleted:**

**Formatted:** Font: Not Bold, Italic

**Formatted:** Heading 1, Line spacing: single

**Formatted:** Line spacing: 1.5 lines

**Deleted:** has been

**Deleted:** in collaboration with the

- Bodélé depression to the Amazon Basin: a case study, *Atmos. Chem. Phys.*, 10(16), 7533–7544, doi:10.5194/acp-10-7533-2010, 2010.
- Bergametti, G., Marticorena, B., Rajot, J. L., Chatenet, B., Féron, A., Gaimoz, C., Siour, G., Coulibaly, M., Koné, I., Maman, A. and Zakou, A.: Dust Uplift Potential in the Central Sahel: An Analysis Based on 10 years of Meteorological Measurements at High Temporal Resolution, *J. Geophys. Res. Atmos.*, 122(22), 12,433–12,448, doi:10.1002/2017JD027471, 2017.
- Bristow, C. S., Drake, N. and Armitage, S.: Deflation in the dustiest place on Earth: The Bodélé Depression, Chad, *Geomorphology*, 105(1), 50–58, doi:10.1016/j.geomorph.2007.12.014, 2009.
- Bristow, C. S., Hudson-Edwards, K. A. and Chappell, A.: Fertilizing the Amazon and equatorial Atlantic with West African dust, *Geophys. Res. Lett.*, 37(14), doi:10.1029/2010GL043486, 2010.
- 10 Bullard, J. E., Harrison, S. P., Baddock, M. C., Drake, N., Gill, T. E., McTainsh, G. and Sun, Y.: Preferential dust sources: A geomorphological classification designed for use in global dust-cycle models, *J. Geophys. Res.*, 116(F4), F04034, doi:10.1029/2011JF002061, 2011.
- Chiapello, I., Bergametti, G., Chatenet, B., Bousquet, P., Dulac, F. and Soares, E. S.: Origins of African dust transported over the northeastern tropical Atlantic, *J. Geophys. Res. Atmos.*, 102(D12), 13701–13709, doi:10.1029/97JD00259, 1997.
- 15 Crouvi, O., Schepanski, K., Amit, R., Gillespie, A. R. and Enzel, Y.: Multiple dust sources in the Sahara Desert: The importance of sand dunes, *Geophys. Res. Lett.*, 39(13), doi:10.1029/2012GL052145, 2012.
- Dansie, A.P., Wiggs, G.F.S. and Thomas, D.S.G.: Iron and nutrient content of wind-erodible sediment in the ephemeral river valleys of Namibia. *Geomorphology*, 290, 335–346, doi:10.1016/j.geomorph.2017.03.016, 2017.
- Drake, N. A., Handley, R., O’Loingsigh, T., Brooks, N. and Bryant, R.: Identifying Saharan dust sources using remote sensing: a comparison of TOMS AI, Meteosat IDDI and a new MODIS Dust Index, 2008.
- 20 FENNEC: SEVIRI DUST RGB, [online] Available from: <http://www.fennec.imperial.ac.uk/> (Accessed 1 July 2016), 2017.
- Formenti, P., Schütz, L., Balkanski, Y., Desboeufs, K., Ebert, M., Kandler, K., Petzold, A., Scheuven, D., Weinbruch, S. and Zhang, D.: Recent progress in understanding physical and chemical properties of African and Asian mineral dust, *Atmos. Chem. Phys.*, 11(16), 8231–8256, doi:10.5194/acp-11-8231-2011, 2011.
- 25 Gebhart, K. A., Schichtel, B. A. and Barna, M. G.: Directional biases in back trajectories caused by model and input data., *J. Air Waste Manag. Assoc.*, 55(11), 1649–62, doi:10.1080/10473289.2005.10464758, 2005.
- Ginoux, P., Prospero, J. M., Gill, T. E., Hsu, N. C. and Zhao, M.: Global-scale attribution of anthropogenic and natural dust sources and their emission rates based on MODIS Deep Blue aerosol products, *Rev. Geophys.*, 50(3),

doi:10.1029/2012RG000388, 2012.

Gross, A., Goren, T., Pio, C., Cardoso, J., Tirosh, O., Todd, M. C., Rosenfeld, D., Weiner, T., Custódio, D. and Angert, A.: Variability in Sources and Concentrations of Saharan Dust Phosphorus over the Atlantic Ocean, *Environ. Sci. Technol. Lett.*, 2(2), 31–37, doi:10.1021/ez500399z, 2015.

- 5 Gross, A., Palchan, D., Krom, M. D. and Angert, A.: Elemental and isotopic composition of surface soils from key Saharan dust sources, *Chem. Geol.*, 442, 54–61, doi:10.1016/j.chemgeo.2016.09.001, 2016.

Harrison, S. P., Kohfeld, K. E., Roelandt, C. and Claquin, T.: The role of dust in climate changes today, at the last glacial maximum and in the future, *Earth-Science Rev.*, 54(1–3), 43–80, doi:10.1016/S0012-8252(01)00041-1, 2001.

- 10 Haywood, J., Francis, P., Osborne, S., Glew, M., Loeb, N., Highwood, E., Tanré, D., Myhre, G., Formenti, P. and Hirst, E.: Radiative properties and direct radiative effect of Saharan dust measured by the C-130 aircraft during SHADE: 1. Solar spectrum, *J. Geophys. Res.*, 108(D18), 8577, doi:10.1029/2002JD002687, 2003.

Hsu, N. C., Tsay, S.-C., King, M. D. and Herman, J. R.: Aerosol Properties Over Bright-Reflecting Source Regions, *IEEE Trans. Geosci. Remote Sens.*, 42(3), 557–569, doi:10.1109/TGRS.2004.824067, 2004.

- 15 Jickells, T. D., An, Z. S., Andersen, K. K., Baker, A. R., Bergametti, G., Brooks, N., Cao, J. J., Boyd, P. W., Duce, R. A., Hunter, K. A., Kawahata, H., Kubilay, N., laRoche, J., Liss, P. S., Mahowald, N., Prospero, J. M., Ridgwell, A. J., Tegen, I. and Torres, R.: Global Iron Connections Between Desert Dust, Ocean Biogeochemistry, and Climate, *Science* (80-. ), 308(5718), 2005.

- 20 Kaufman, Y. J., Tanré, D., Remer, L. A., Vermote, E. F., Chu, A. and Holben, B. N.: Operational remote sensing of tropospheric aerosol over land from EOS moderate resolution imaging spectroradiometer, *J. Geophys. Res. Atmos.*, 102(D14), 17051–17067, doi:10.1029/96JD03988, 1997.

Kaufman, Y. J., Koren, I., Remer, L. A., Tanré, D., Ginoux, P. and Fan, S.: Dust transport and deposition observed from the Terra-Moderate Resolution Imaging Spectroradiometer (MODIS) spacecraft over the Atlantic Ocean, *J. Geophys. Res.*, 110(D10), D10S12, doi:10.1029/2003JD004436, 2005.

- 25 Kim, D., Chin, M., Remer, L. A., Diehl, T., Bian, H., Yu, H., Brown, M. E. and Stockwell, W. R.: Role of surface wind and vegetation cover in multi-decadal variations of dust emission in the Sahara and Sahel, *Atmos. Environ.*, 148, 282–296, doi:10.1016/J.ATMOENV.2016.10.051, 2017.

Klose, M., Shao, Y., Karremann, M. K. and Fink, A. H.: Sahel dust zone and synoptic background, *Geophys. Res. Lett.*, 37(9), doi:10.1029/2010GL042816, 2010.

Knippertz, P. and Todd, M. C.: Mineral dust aerosols over the Sahara: Meteorological controls on emission and transport and



implications for modeling, *Rev. Geophys.*, 50(1), RG1007, doi:10.1029/2011RG000362, 2012.

Koren, I., Kaufman, Y. J., Washington, R., Todd, M. C., Rudich, Y., Martins, J. V. and Rosenfeld, D.: The Bodélé depression : a single spot in the Sahara that provides most of the mineral dust to the Amazon forest, *Env. Res. Lett.*, 1, 14005–5, doi:10.1088/1748-9326/1/1/014005, 2006.

- 5 Lensky, I. M. and Rosenfeld, D.: Clouds-Aerosols-Precipitation Satellite Analysis Tool (CAPSAT), *Atmos. Chem. Phys.*, 8(22), 6739–6753, doi:10.5194/acp-8-6739-2008, 2008.

Levy, R. C., Mattoo, S., Munchak, L. A., Remer, L. A., Sayer, A. M., Patadia, F. and Hsu, N. C.: The Collection 6 MODIS aerosol products over land and ocean, *Atmos. Meas. Tech.*, 6(11), 2989–3034, doi:10.5194/amt-6-2989-2013, 2013.

- 10 Mahowald, N. M., Bryant, R. G., del Corral, J. and Steinberger, L.: Ephemeral lakes and desert dust sources, *Geophys. Res. Lett.*, 30(2), doi:10.1029/2002GL016041, 2003.

- Mahowald, N. M., Kloster, S., Engelstaedter, S., Moore, J. K., Mukhopadhyay, S., McConnell, J. R., Albani, S., Doney, S. C., Bhattacharya, A., Curran, M. A. J., Flanner, M. G., Hoffman, F. M., Lawrence, D. M., Lindsay, K., Mayewski, P. A., Neff, J., Rothenberg, D., Thomas, E., Thornton, P. E. and Zender, C. S.: Observed 20th century desert dust variability: impact on climate and biogeochemistry, *Atmos. Chem. Phys.*, 10, 10875–10893, doi:10.5194/acp-10-10875-2010, 15 2010.

Moulin, C. and Chiapello, I.: Impact of human-induced desertification on the intensification of Sahel dust emission and export over the last decades, *Geophys. Res. Lett.*, 33(18), doi:10.1029/2006GL025923, 2006.

Muhs, D. R., Prospero, J. M., Baddock, M. C. and Gill, T. E.: Identifying Sources of Aeolian Mineral Dust : Present and Past., 2014.

- 20 Prospero, J. M., Ginoux, P., Torres, O., Nicholson, S. E. and Gill, T. E.: Environmental characterization of global sources of atmospheric soil dust identified with the NIMBUS 7 Total Ozone Mapping Spectrometer (TOMS) absorbing aerosol product, *Rev. Geophys.*, 40(1), 1002, doi:10.1029/2000RG000095, 2002.

Ridley, D. A., Heald, C. L. and Ford, B.: North African dust export and deposition: A satellite and model perspective, *J. Geophys. Res. Atmos.*, 117(D2), doi:10.1029/2011JD016794, 2012.

- 25 Sayer, A.M., Hsu, N.C., Bettenhausen, C., Jeong, M.-J.: Validation and uncertainty estimates for MODIS Collection 6 “Deep Blue” aerosol data, *J. Geophys. Res. Atmos.*, 118(14), doi:10.1002/jgrd.50600, 2013.

Schepanski, K., Tegen, I., Laurent, B., Heinold, B. and Macke, A.: A new Saharan dust source activation frequency map derived from MSG-SEVIRI IR-channels, *Geophys. Res. Lett.*, 34(18), L18803, doi:10.1029/2007GL030168, 2007.

Deleted: .....Page Break.....  
¶

Schepanski, K., Tegen, I., Todd, M. C., Heinold, B., Bönisch, G., Laurent, B. and Macke, A.: Meteorological processes forcing Saharan dust emission inferred from MSG-SEVIRI observations of subdaily dust source activation and numerical models, *J. Geophys. Res.*, 114(D10), D10201, doi:10.1029/2008JD010325, 2009.

Schepanski, K., Tegen, I. and Macke, A.: Comparison of satellite based observations of Saharan dust source areas, *Remote Sens. Environ.*, 123, 90–97, doi:10.1016/j.rse.2012.03.019, 2012.

Scheuvsen, D., Schütz, L., Kandler, K., Ebert, M. and Weinbruch, S.: Bulk composition of northern African dust and its source sediments — A compilation, *Earth-Science Rev.*, 116, 170–194, doi:10.1016/J.EARSCIREV.2012.08.005, 2013.

Swap, R., Garstang, M., Greco, S., Talbot, R. and Kållberg, P.: Saharan dust in the Amazon Basin, *Tellus*, 44B(2), 133–149, doi:10.1034/j.1600-0889.1992.t01-1-00005.x, 1992.

10 Tegen, I., Harrison, S. P., Kohfeld, K., Prentice, I. C., Coe, M. and Heimann, M.: Impact of vegetation and preferential source areas on global dust aerosol: Results from a model study, *J. Geophys. Res. Atmos.*, 107(D21), AAC 14-1-AAC 14-27, doi:10.1029/2001JD000963, 2002.

Washington, R., Todd, M., Middleton, N. J. and Goudie, A. S.: Dust-Storm Source Areas Determined by the Total Ozone Monitoring Spectrometer and Surface Observations, *Ann. Assoc. Am. Geogr.*, 93(2), 297–313, doi:10.1111/1467-8306.9302003, 2003.

15 Yu, H., Chin, M., Yuan, T., Bian, H., Remer, L. A., Prospero, J. M., Omar, A., Winker, D., Yang, Y., Zhang, Y., Zhang, Z. and Zhao, C.: The fertilizing role of African dust in the Amazon rainforest: A first multiyear assessment based on data from Cloud-Aerosol Lidar and Infrared Pathfinder Satellite Observations, *Geophys. Res. Lett.*, 42(6), 1984–1991, doi:10.1002/2015GL063040, 2015.

20

### Appendix i: Examples of geomorphic classes

In the figures below, examples of the various geomorphic classes used in this study can be found. In order, the geomorphic categories are: paleolake (Figure 5), alluvial deposit (Figure 6), stony surface (Figure 7), sand deposit (Figure 8), and anthropogenic (Figure 9).

5

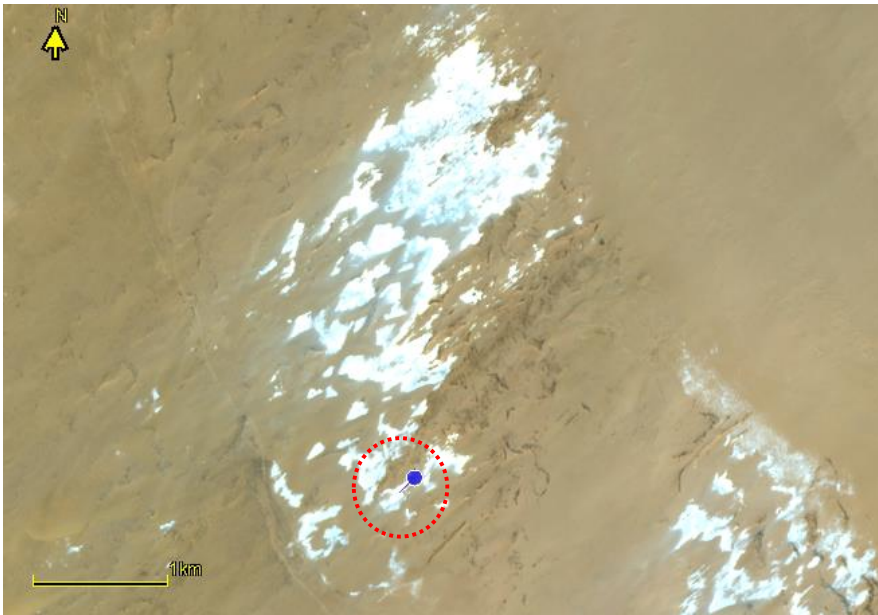
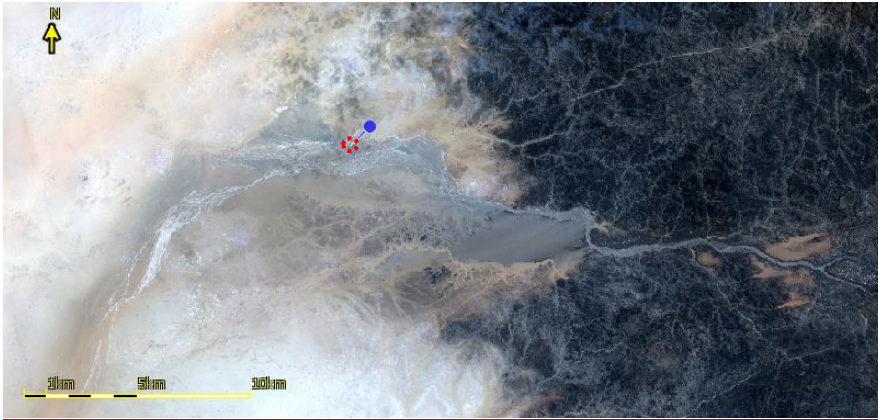
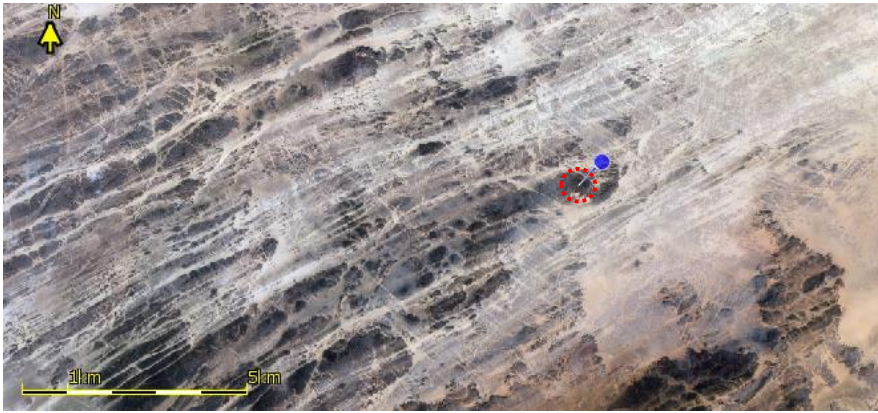


Figure 5: Sentinel-2 natural colour composite showing a diatomite paleolake in the Bodélé Depression region, Chad, identified as a dust source. This source emitted dust on the 23<sup>rd</sup> of December 2015. Location of the pin in lat, long: 17.4875, 19.4845. 750m buffer included in red.

10



**Figure 6:** Sentinel-2 natural colour composite showing an alluvial deposit dust source west of the Tibesti mountains in Chad. The source emitted dust on the 30<sup>th</sup> of November 2015. Location of the pin in lat, long: 21.4001, 15.8211. 750m buffer included in red.



**Figure 7:** Sentinel-2 natural colour composite showing a stony surface dust source near the border between Chad and Niger in the North. The source emitted dust on the 1st of December 2015. Location of the pin in lat, long: 22.2030, 15.2052. 750m buffer included in red.



**Figure 8:** Sentinel-2 natural colour composite showing a sand deposit (barchan dune) dust source, ~35 km northeast of Faya-Largeau, Chad. This source emitted dust on the 23<sup>rd</sup> of December 2015. Location of the pin in lat, long: 17.4655, 19.6163. 750m buffer included in red.

5



**Figure 9:** Sentinel-2 natural colour composite showing two anthropogenic dust sources in Sudan. The agricultural dust source (blue pin) emitted dust on the 21<sup>st</sup> of February 2016. Location of the blue pin in lat, long: 18.7989, 30.4026. The village dust source (red pin) emitted dust on the 26<sup>th</sup> of January 2016. Location of the red pin in lat, long: 18.8448, 30.4776. 750m buffer included in dotted red.

10